
CMS Conference Report

Radiation damage effect on Avalanche Photodiodes

S. Baccaro¹, J.E. Bateman², F. Cavallari³, V. Da Ponte⁴, K. Deiters⁵, P. Denes⁶, M. Diemoz³, Th. Kirm⁷, A.L. Lintern², E. Longo³, M. Montecchi¹, Y. Moussienko^{8,a}, J.P. Pansart⁴, D. Renker⁵, S. Reucroft⁸, G. Rosi¹, R. Rusack⁹, D. Ruuska⁸, R. Stephenson², M.J. Torbet²

(Talk given by F. Cavallari at the 2nd International Conference on Radiation Effects on Semiconductor Materials, Detectors and Devices, March 4-6, 1998, Firenze)

Abstract

Avalanche Photodiodes have been chosen as photon sensors for the electromagnetic calorimeter of the CMS experiment at the LHC. These sensors should operate in the 4 T magnetic field of the experiment.

Because of the high neutron radiation in the detector extensive studies have been done by the CMS collaboration on the APD neutron radiation damage. The characteristics of these devices after irradiation have been analyzed, with particular attention to the quantum efficiency and the dark current.

The recovery of the radiation induced dark current has been studied carefully at room temperature and at slightly lower and higher temperatures. The temperature dependence of the defects decay-time has been evaluated.

¹) ENEA-Casaccia, S. Maria di Galeria, and INFN, Sezione di Roma, Italy

²) Rutherford Appleton Laboratory, Chilton, Didcot, U.K.

³) Università di Roma "La Sapienza" and INFN, Sezione di Roma, Italy

⁴) DSM/DAPNIA, CEA/Saclay, Gif-sur-Yvette, France

⁵) Paul Scherrer Institut, Villigen, Switzerland

⁶) Princeton University, Princeton, USA

⁷) RWTH, I. Physikalisches Institut, Aachen, Germany

⁸) Northeastern University, Boston, USA

⁹) University of Minnesota, Minneapolis, USA

^a) On leave from Institute for Nuclear Research, Moscow, Russia

1 Introduction

Avalanche photodiodes have been chosen as photon sensors for the PbWO_4 crystals of the electromagnetic calorimeter of CMS [1] in the barrel region. The choice of these sensors is motivated by the low light yield of the crystals, which demands sensors with some internal amplification, and by the high magnetic field inside the experiment (4 Tesla) which excludes the use of photomultipliers.

Since two years there has been a strong R&D collaboration with two firms (Hamamatsu and EG&G) to produce suitable detectors. The scintillating light of the crystals is peaked around 430 nm and thus the quantum efficiency of the prototypes in use has been optimized for this wavelength. The Nuclear Counter Effect (see Section 2.1) has been decreased and the radiation hardness of the detectors has been improved.

The drawback is that the area of the detectors from both the firms is of 0.25 cm^2 , which represents only 4 % of the endface of each crystal. Thus two APDs per each crystal will be mounted.

2 Properties of Avalanche Photodiodes

The structure and working principle of these avalanche photodiodes is described in [2]. The methods used by the two firms for the production of the APDs is epitaxial growth for the Hamamatsu and ion diffusion and implantation for the EG&G. The doping profiles and other characteristics are known in general, being the details industrial secrets of the two firms.

The characteristics which are relevant for the operation of these sensors in CMS are the stability of the gain with respect to temperature and bias changes (which could affect the calibration of the detector), the quantum efficiency and excess noise factor (which enter directly in the stochastic term of the energy resolution of the detector) and the induced electronic noise. A summary of these parameters for the two firms is indicated in [2].

The noise of the photon detector and the associated electronics is given by two terms: a parallel noise term and a series noise term. The first is given by the thermal noise in the APD series resistance and in the preamplifier, and it is governed by the capacitance of the device. The second term is caused by the APD dark current and it is proportional to the square root of the dark current and the shaping time τ of the shaper.

For the APD's it is useful to distinguish the dark current I_D in two terms: a surface current I_S and a bulk current I_B , the latter being more important because it is multiplied by the gain.

2.1 Nuclear Counter Effect

Charged particles leaking from the crystals in a high energy electromagnetic shower can cause a signal in the APD if they cross it. This effect is known as Nuclear Counter Effect and, for low light-yield crystals, it can seriously spoil the energy resolution of the calorimeter, causing a tail on the high energy side of the response.

The parameter which is relevant for this aspect is the *effective thickness* of the APD. This is the thickness of a silicon PIN diode required to give the same signal (in terms of photoelectrons) when traversed by a charged particle. It can be measured by comparison of the charge given by electrons from a radioactive source in the APD divided by the gain of the device and the charge collected in a conventional PIN photodiode divided by its thickness.

The deterioration of the energy resolution due to this effect was indeed observed in the test-beam for the first calorimeter prototypes while it is no more present in the new prototypes, which have longer crystals and APD with a smaller effective thickness.

3 Radiation Damage

The fluence of neutrons and the gamma dose in the barrel region of the calorimeter have been calculated in [2]. The fluence which corresponds to 10 year of operation of the LHC with an integrated luminosity of $5 \cdot 10^5 \text{ pb}^{-1}$ is $2 \cdot 10^{13} \text{ neutrons/cm}^2$, while the gamma dose has been estimated to be 3-5 kGy.

The radiation effect on the APD's is twofold:

- the surface damage, mainly caused by gammas, can deteriorate the quantum efficiency and increase the surface current;
- the neutron damage causes defects in the silicon bulk which induce an increase in the dark current of the detector and thus in the noise.

The effect of the gamma radiation has been studied in [3]. There it has been established that the old prototypes, which had a front window made of SiO_2 , show a decrease of the quantum efficiency in the short wavelength region

after γ irradiation, while the new prototypes, with a Si_3N_4 window, show no change in the quantum efficiency after exposure to a ^{60}Co source up to a dose of 55 kGy.

At this level of fluence, the main problem is caused by the neutron radiation. The main consequence of the neutron damage is the increase of the dark current in the detector.

Figure 1 shows the increase in the bulk current as a function of the neutron fluence Φ . It can be noticed that the increase of the bulk current grows linearly with the fluence.

The creation of the defects in the silicon lattice which are responsible for the increase of the dark current is a volume effect, so usually the increase in the dark current I_D is written as:

$$I_D = \alpha V \Phi \quad (1)$$

where V is the volume of the detector and α is a parameter which has been measured by different groups, see for instance [4] and its value is:

$$\alpha \simeq (8 - 10)10^{-17} \text{ A/cm}$$

for 1 MeV neutrons, at 18°C and after 2-3 days from the irradiation.

In the case of Avalanche Photodiodes, the volume which is relevant for the generation of the bulk current is the area times the effective thickness of the detector. In fact this gives a measurement of the α parameter which is slightly higher but consistent with the measurements found in literature for diodes:

$$\alpha \simeq (10 - 13)10^{-17} \text{ A/cm.}$$

The effective thickness is of the order of 5 μm for the Hamamatsu APDs and 7-10 μm for the EG&G APDs, this is the reason why these devices are more radiation hard than conventional PIN photodiodes, for which the volume would be given by the area times the whole thickness of the detector (typically 200 μm).

The effective thickness is inversely proportional to the capacitance of the device. Furthermore the thickness of the conversion layer of the APD (the region where the photons are converted into electrons), which is part of the effective thickness, must be optimized for the wavelength of the PbWO_4 . So a decrease of the effective thickness improves the performance of the detector for what concerns the N.C.E. and the radiation damage, but it increases the capacitance and could influence the quantum efficiency. A compromise must be found between these effects in order to optimize the total noise.

4 Annealing studies

It is very important to understand the long-term annealing of these devices, because the data-taking period of the LHC experiments will last 10 years with 6 months of data-taking and 6 months of shutdown per year.

The recovery of the dark current can be described [5] as a sum of exponentials, each exponential being attributed to the recovery of one defect with its proper recovery-time τ_i and its weight g_i .

$$\frac{I_D(t)}{I_D(0)} = \sum_i g_i e^{-t/\tau_i}$$

Figure 2 shows the recovery of the dark current of an APD irradiated to $1.4 \cdot 10^{12} \text{ n/cm}^2$. The measurements start after 1-2 days from the irradiation, so they are not sensitive to the very fast components of the decay. Table 1 shows the decay-time and the contribution of the various components fitted from these data points. Several other APDs have been irradiated with neutrons and protons with the same total dose and show similar behaviour (see [6] and [7]).

Since it is expected that τ depends on the temperature, the same fit has been done for two other APDs whose recovery has been followed respectively at 0°C and 12°C. Figure 3 shows the recovery of these two devices. Figure 4 shows the recovery of an APD which has been irradiated to $4 \cdot 10^{13} \text{ n/cm}^2$ and has been held at room temperature for 180 days after the irradiation. Then the temperature was increased to 38°C for 20 days. In this phase evidence for a new fast recovery is observed. To check that this recovery was indeed triggered by the temperature, the APD was again held at room temperature for 45 days and no recovery was observed. Then the temperature was increased to 45°C and subsequently to 55-60°C. The various parameters of the fits are summarized in Table 1 (for more details see [8]).

Figure 5 summarizes the various decay times observed in these devices.

In [9] the temperature dependence of the recovery-time τ of defects is parametrized as:

$$\tau = \theta e^{E/K_B T}, \quad (2)$$

where K_B is the Boltzmann constant and T is the temperature in degrees Kelvin. It can be concluded that, beside the first fast component, which was not detectable, there is evidence for two other components, with parameters:

$$E_2=(0.95\pm 0.01)\text{ eV} \quad \theta_2 = (7.9 \pm 1.5) \cdot 10^{-16} \text{ days}$$

$$E_3=(0.45\pm 0.01)\text{ eV} \quad \theta_3 = (2.2 \pm 1.0) \cdot 10^{-6} \text{ days}$$

The component 2 was also observed in [9] and the release energy is compatible with those measurements.

The component 3 gives a very long decay-time at room-temperature which can be slightly increased at higher temperatures. However, the relative weight of this component is very small compared to the others, of the order of 10 %.

It is very difficult from these fits to establish firmly the presence of the component 4, (the open stars in Figure 5), because the decay-time is very low and the weight of the component is very small. This would require an observation of the recovery for few years at room-temperature.

With the measured parameters for the damage and recovery of the dark current and the foreseen schedule of the machine, it is possible to calculate the expected noise induced by the radiation in these devices to about 70 MeV per crystal after 10 years of operation (see [6]), which is within the CMS prescriptions.

5 Conclusions

The gamma and neutron radiation damage on the APDs has been studied by the CMS-ECAL collaboration in order to prove their applicability for the experiment.

The characteristics of these devices are now satisfactory for what concerns their use in the calorimeter.

The dark current annealing has been measured at room temperature and at slightly lower and higher temperatures and several components of the recovery have been found. In particular two components have been observed: a medium term one (of the order of 10 days at room temperature) and a very long one (of the order of 100 days).

Further measurements are required to assess the presence of other components.

These measurements have allowed an estimate of the radiation-induced noise given by these devices to 70 MeV per crystal after 10 years of operation, which is within the CMS prescriptions.

References

- [1] CMS, *The Compact Muon Solenoid, Technical Proposal*, CERN/LHCC 94-38.
- [2] CMS, *The Electromagnetic Calorimeter Project, Technical Design Report*, CERN/LHCC 97-33 (15 Dec. 1997).
- [3] Th. Kirn *et al.*, Nucl. Instr. and Meth. A387 (1997) 202.
- [4] M. Bosetti, C. Furetta, C. Leroy, S. Pensotti, P.G. Rancoita, M. Rattaggi, M. Redaelli, M. Rizzatti, A. Seidman, G. Terzi, *Effect on charge collection and structure of n-type silicon detectors irradiated with large fluences of fast neutrons*, Nucl. Instr. and Meth. A 343 (1994) 435.
- [5] B. Borchi, M. Bruzzi, *Radiation damage in silicon detectors*, Riv. del N. Cim., vol. 17, N.11 (1994).
- [6] S. Baccaro, *et al.*, *APD Properties and Recovery from Radiation damage*, CMS Note 1997/030.
- [7] J.E. Bateman, *et al.*, *Fast Neutron irradiation of some APDs proposed for application in the CMS ECAL*, RAL-TR-97-075.
- [8] S. Baccaro, *et al.*, *Radiation Damage studies on APDs*, CMS Note in preparation.
- [9] V. Eremin, A. Ivanov, E. Verbitskaya, Z. Li, H.W. Kraner, *Elevated Temperature annealing of the neutron induced reverse current and corresponding defect levels in low and high resistivity silicon detectors*, IEEE Trans. Nucl. Sci. 42 (1995) 387.

APD	Fit	g_1	τ_1 (d)	g_2	τ_2 (d)	g_3	τ_3 (d)	g_4	τ_4 (d)	T(°C)
BC-24	3e+c	0.35	1.27 (fixed)	0.26	6.7±1.0	0.17	69±5	0.22	∞	~20
BC-PS	3e+c	0.31	1.27 (fixed)	0.27	13.4±0.2	0.08	98±5	0.34	∞	21
BC-25 I	e+c	0.35	4.1 ± 1.0	0.204	–	–	–	0.796	∞	0
BC-25 II	e+c	0.35	–	0.35	10±1	0.146	160±20	0.30	∞	~20
CC-02	2e+c	0.08	1.4 ± 3.0	0.43	45.5±7	–	–	0.49	∞	12
APD	Fit	g_2	τ_2 (d)	g_3	τ_3 (d)	g_4	τ_4 (d)	g_5	τ_5 (d)	T(°C)
BD-5 I	2e+c	0.05	2.5±0.5	0.25	40± 2	0.70	∞	–	–	~38
BD-5 II	2e+c	–	–	0.25	31± 7	0.17	860±200	0.53	∞	45-50
BD-5 III	e+c	–	–	–	–	0.17	80±10	0.53	∞	~60

Table 1: For each APD the Table shows the type of fit used for the annealing, the estimated parameters and the temperature at which the recovery took place.

(e = exponential, c = constant) In Figure 5 for the room temperature data, the points in the plot refer to the APD BC-PS, because the temperature during the recovery was controlled more carefully.

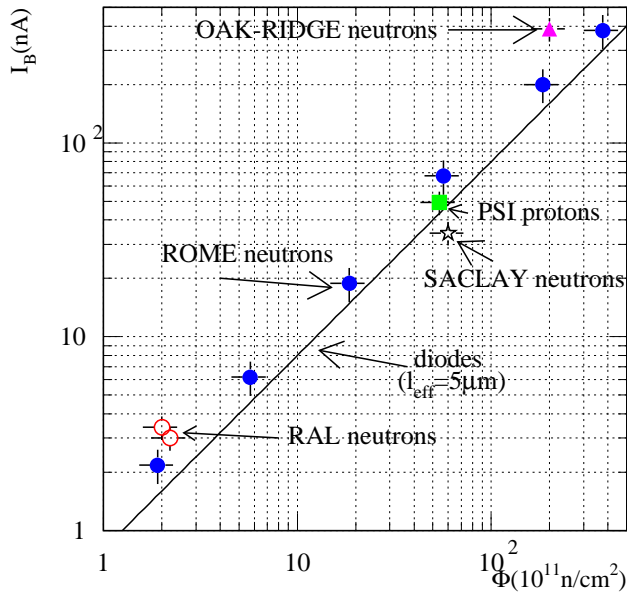


Figure 1: Radiation induced bulk current versus dose for one of the Hamamatsu APDs. The measurements were done at 18°C and after 2 days from the irradiation. The curve labelled *diodes* shows what would be the damage for a simple diode 5 μm thick according to Eq. (1).

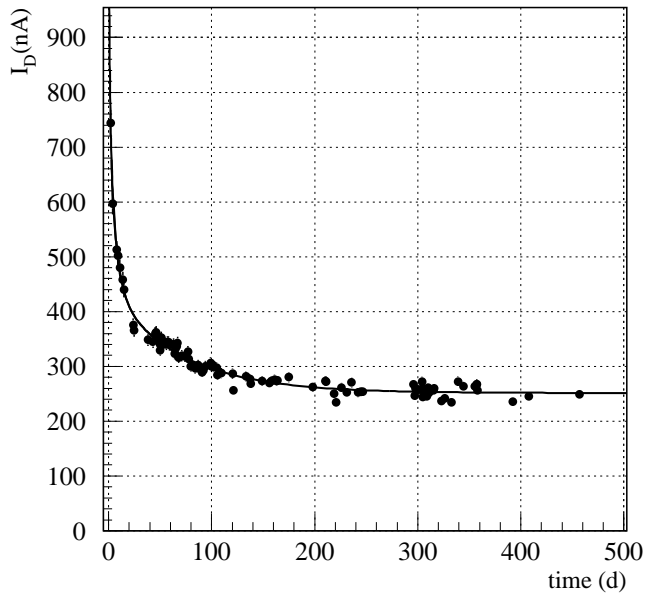
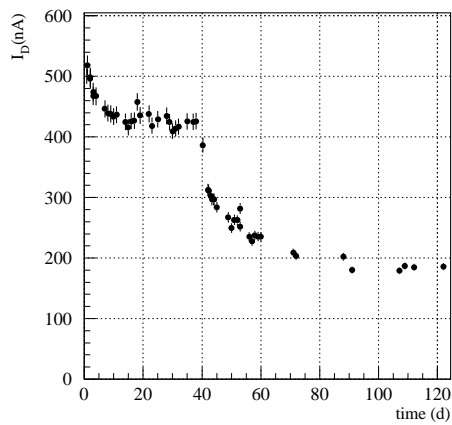
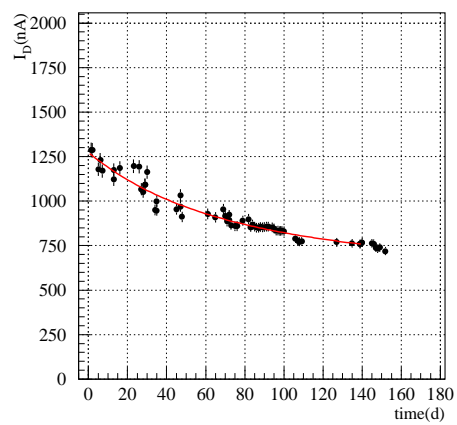


Figure 2: Room temperature annealing of the dark current of one of the Hamamatsu APDs (type BC-24), irradiated at the Tapiro reactor at ENEA with a dose of $1.4 \cdot 10^{12} \text{ n/cm}^2$. The measurements were done at a gain of 50 and at room temperature, but they were rescaled at 18°C .



(a)



(b)

Figure 3: Low temperature annealing of the dark current of two Hamamatsu APDs: type BC-25 (a) and type CC-02 (b), irradiated at the Tapiro reactor at ENEA with a dose respectively of $4.9 \cdot 10^{11}$ and $1 \cdot 10^{12} \text{ n/cm}^2$. APD BC-25 (a) was held at 0°C for 40 days and then at room temperature, while ADP CC-02 (b) was held at 12°C . The measurements were done at a gain of 50 but they were rescaled all at 18°C .

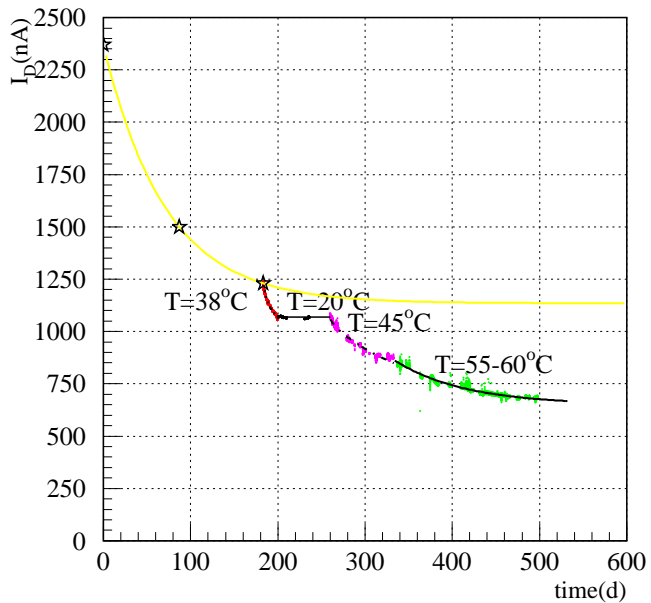


Figure 4: Recovery of the dark current of the APD Hamamatsu BD-5. The first part (indicated by the open stars) was at room temperature, then the APD was held at 38°C, at room temperature again and at higher temperatures, as indicated in the plot.

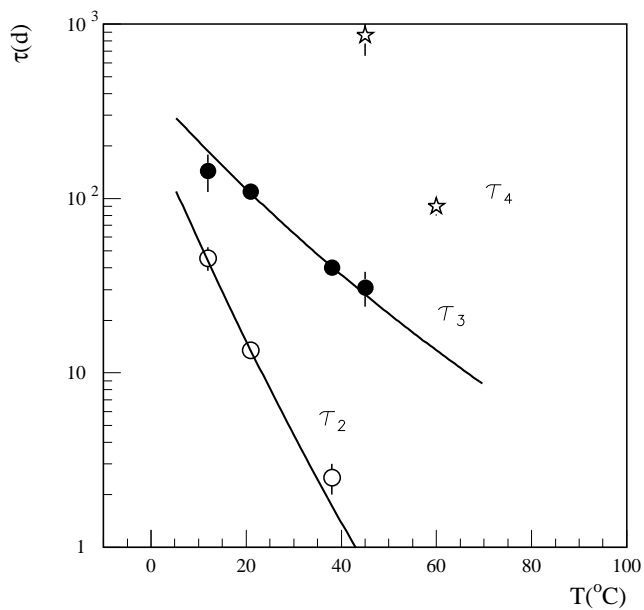


Figure 5: Temperature dependence of the decay-time of the various components of the dark current as in Table 1. The components numbered as 2 and 3 are well established from the fits to the data, while the component numbered as 4 cannot be firmly established.